BULLETIN OF THE POLISH ACADEMY OF SCIENCES
TECHNICAL SCIENCES
Vol. 54, No. 2, 2006

Formation of texture inhomogeneity in severely plastically deformed copper

I.V. ALEXANDROV[1*], M.V. ZHILINA[1], and J.T. BONARSKI[2]

[1]Ufa State Aviation Technical University, 12 K. Marx St., Ufa, Russia
[2]Institute of Metallurgy and Materials Science, Polish Academy of Sciences, 25 Reymonta St., 30-059 Kraków, Poland

Abstract. The development of the crystallographic texture in copper subjected to severe plastic deformation (SPD) by means of high pressure torsion (HPT) and equal-channel angular pressing (ECAP) was experimentally investigated and analyzed by means of computer modelling. It was demonstrated, that the texture developed in HPT and ECAP Cu is characterized by significant inhomogeneity. Therefore, the analysis focused on the study of the texture distribution and its inhomogeneity in sample space. The detailed texture analysis, based on the X-ray diffraction technique, led to important observations concerning the localization of the maximum texture gradient and the regularity of its changes related to the parameters of the applied deformation. The obtained results provided the basis for certain conclusions concerning complex texture changes in SPD Cu.

Key words: severe plastic deformation, crystallographic texture, texture homogeneity.

1. Introduction

Recently, numerous investigations have successfully demonstrated the unique potential of the severe plastic deformation (SPD) technique for formation of ultra-fine grained and nanostructured materials, when applied to different metals and alloys in bulk form [1]. However, the SPD process is accompanied by the formation of high-angle grain boundaries, characterized by various orientation vectors as well as developed crystallographic texture [2,3]. The creation of such a structure resulted in the intensification of mechanical and physical properties of numerous metals and their alloys. It is known, that crystallographic texture of metals reflects the most microstructural changes that occurred during the deformation process. Studying texture is very useful for the understanding of the SPD deformation mechanisms and for determining texture-sensitive properties.

The most popular SPD technique is the so-called equal-channel angular pressing (ECAP), which is well described in the literature [1,4]. Depending on the mode of pressing (deformation route) and the number of passes, the achieved degree of deformation can be relatively high. One ECAP-passing results only in the deformation of $\varepsilon \approx 1.15$ using a 90° tool [5]. The character of the spatial arrangement of crystals (and generated grains) formed during the ECAP-passing changes with each pressing cycle. However, the arrangement formed during the first ECAP-passing has a tendency to be preserved to some extent in the following cycles. On the other hand, similar microstructural effects can be achieved by the so-called high pressure torsion (HPT), a type of the SPD, which is more and more frequently applied to obtain nano-structured materials [6–10]. The HPT process is at continuous deformation mode and allows to achieve high degrees of deformation ($\varepsilon > 100$).

According to the published works [3,11–20], textures formed during the SPD process exhibit features of simple shearing [21] with the presence of other types of components, while they lack orthorhombic or axial sample symmetry. Thereby, the interpretation of experimental results usually requires additional information on the microstructure and/or distribution of mechanical properties of the examined materials. Among the reasons for the above mentioned "picture" of texture of the material exposed to SPD, one finds strong inhomogeneity of the deformation field (plastic flow) [22] moderated by compressive and tensile stresses during the process [16]. In this context, computer modelling of crystallographic texture development becomes very promising, as it can take into account the complicated character of the stress-strain state of materials [23–25].

The current paper presents the results of recent investigations, aimed to reveal the crystallographic texture evolution mechanisms during SPD and performed experimentally and by means of 3D simulation of ECAP and HPT in pure Cu (99.98%) with initially near-random distribution of orientations. The goal of the work is to present texture changes during the SPD process.

2. Method and materials

The texture analysis was conducted on the basis of the X-ray diffraction technique. The adequate back-reflection pole figures $P_{(hkl)}(\alpha, \beta)$ were registered in the range of the pole angle α varying from 0° to 75° and the azimuthal angle β – from 0° to 360°. The measurements were performed with the Philips X'Pert system, equipped with the texture goniometer ATC-3. The filtered X-ray radiation CuKα (λ = 0.154183 nm) was used. The applied collimated incident beam had a diameter

*e-mail: iva@mail.rb.ru

of 0.6 mm. It means, that each marked measurement point is representative for the indicated area of the examined samples, representing both the ECAP- and HPT-processed material (see Fig. 1).

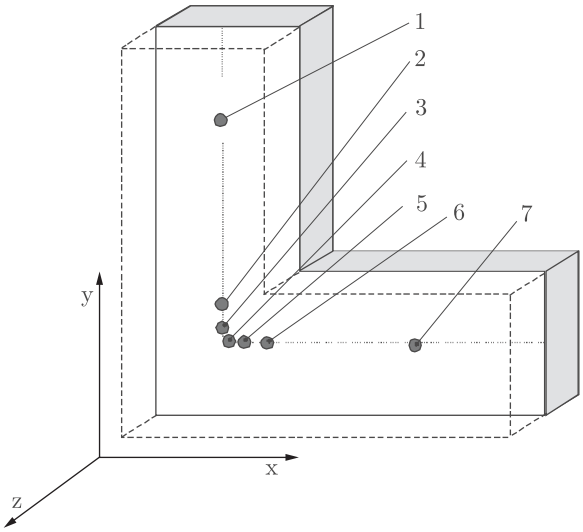

Fig. 1. Scheme of the longitudinal section of the examined ingot of Cu, subjected to ECAP. The texture measurements were performed in the section areas marked by points 1 to 7

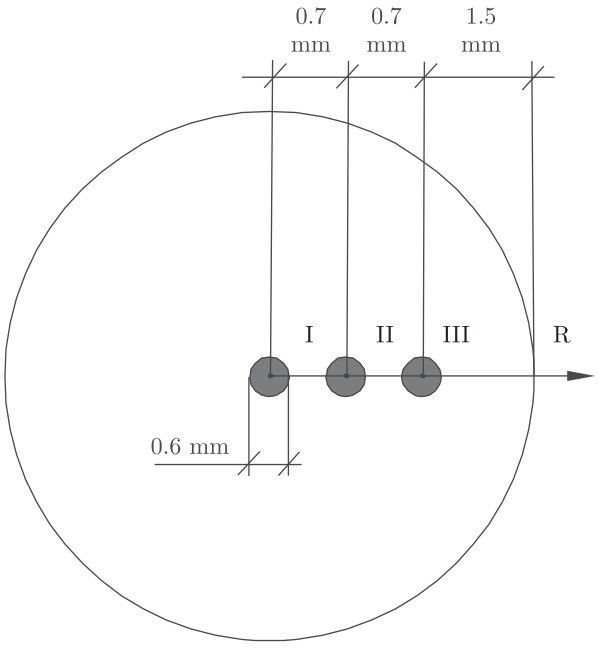

Fig. 2. Distribution of HPT-sample areas (I, II, III), where the texture measurements were performed

ECAP details. The size of Cu (99.98%) billets subjected to ECAP with a deformation rate of 6 mm/s at ambient temperature was 60·8·8 mm. The angle of the channels' intersection was 90°. This paper presents the study of the homogeneity of the crystallographic texture after the treatment by ECAP along route B_C (90° clock-wise rotations of the ingot around its longitudinal axis between the passes). The presented results concern the longitudinal- and cross sections (see Fig. 1) of the processed ingot, where experimental data were collected (Fig. 9).

HPT details. A slice-shaped processed Cu (99.98%) sample (10 mm in diameter and 0.7 mm in thick) was located between two (top and bottom) cylindrical heads of a mechanical press. One of the heads (bottom) was rotated in the plane perpendicular to its axis, while a compression force (up to 5 GPa) was simultaneously applied to the sample. Due to friction forces between the sample and the heads' surfaces, both compression and shearing processes of the examined material in the state of a condition quasi-hydrostatic were realized during the HPT. The deformation was realized at ambient temperature for varying numbers of rotations: 1, 5 and 10. For each of the three cases, the rate of compression was equal to 0.35 mm/s and the rate of rotation was 0.11 rad/s. The investigation of the crystallographic texture was conducted according to the scheme presented in Fig. 2.

The computer simulation of texture development was performed for the ECAP mode of the Cu sample. Suitable calculations considered the visco-plastic self-consistent model [21], the deformation strength was realized by the Voce model [26]. The original texture was represented by 830 single orientations, grouped in several components related to the experimentally-identified texture and its volume fractions for the Cu ingot before processing. The input parameters for the texture evolution modelling were the tensor components of the strain rate gradient. As a result, the calculations yield the differential of the tensor component of temporary and accumulated strain for each point of the selected trajectory of the plastic flow of the material [23]. The calculation procedures were performed by means of the DRAKON package [27]. LaboTex software was used to build pole figures (PFs), orientation distribution functions (ODFs) and to perform quantitative analysis of the obtained results [28].

3. Results and discussion

3.1. Texture evolution in HPT process. The experimental PF of 111 planes of the Cu sample after HPT by 1-, 5- and 10-rotations for each investigated areas (points: I, II, III) are given in Fig. 3

The general distribution of the dominating texture components given in the PF presented in Fig. 3 can be characterized by three zones of cumulated intensities of the 111 poles. The first zone is located in the centre of the PF. The second one has the form of a ring, co-centred with the pole figure area. There can be observed two symmetrically located areas of the ring with much more intensity. The third zone, in which the PF intensity consists of two symmetrical areas, appeared in most cases in the peripheral region of the figures. The central points of the zones (identical with the PF centre) for each of the measurement sample area showed a tendency to its tilting. The same effect was identified in the related ODFs, one of which is presented in Fig. 4.

To interpret the identified texture, it is advisable to compare it with the pure shearing texture described by ideal components given in Tab. 1. As it is shown in Fig. 4, two texture fibres are formed during the HPT process, namely: {111}<uvw> and

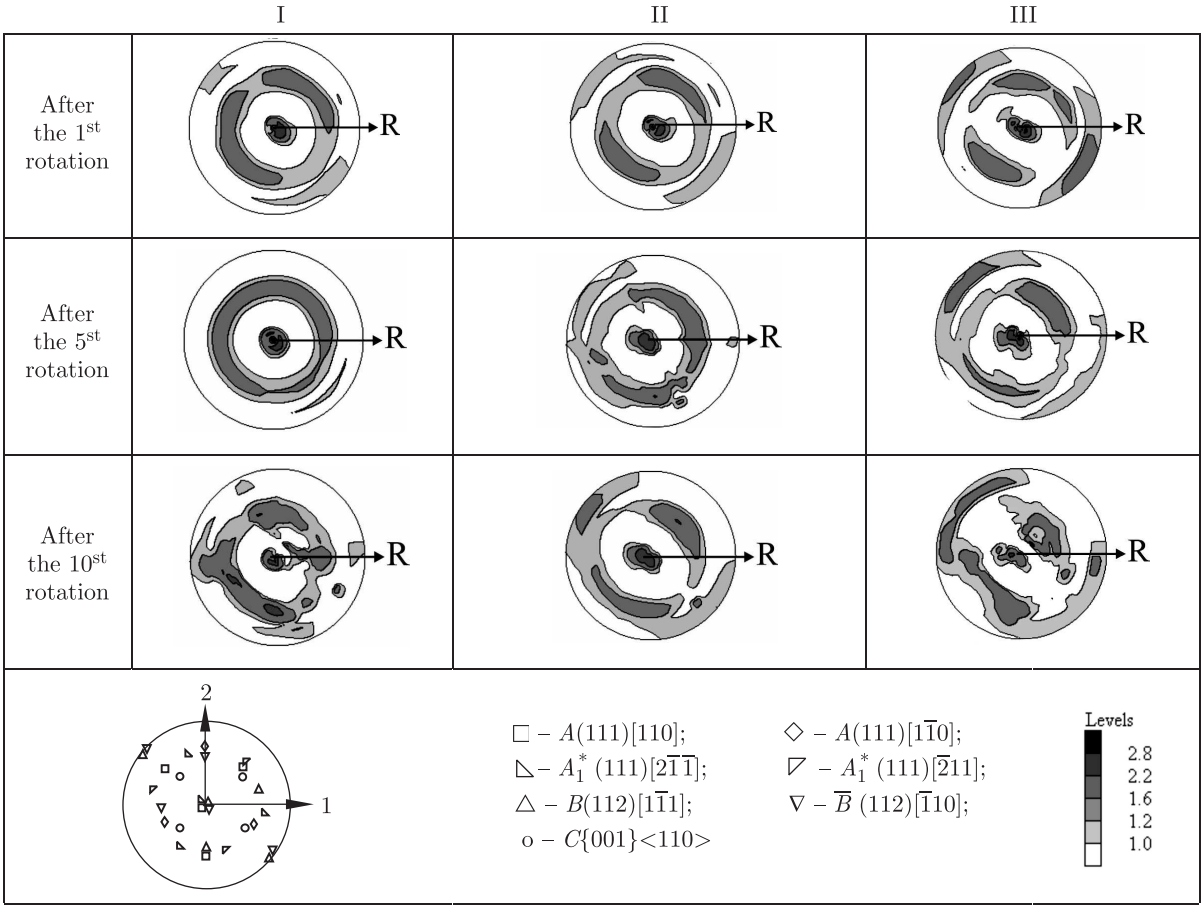

Fig. 3. Experimental PF (111) for Cu-sample after HPT process consisting of 1-, 5- and 10 rotations in the selected areas (I, II and III) marked in Fig. 2. The bottom row presents a model pole figure (111) with the positions of ideal orientations of simple shear

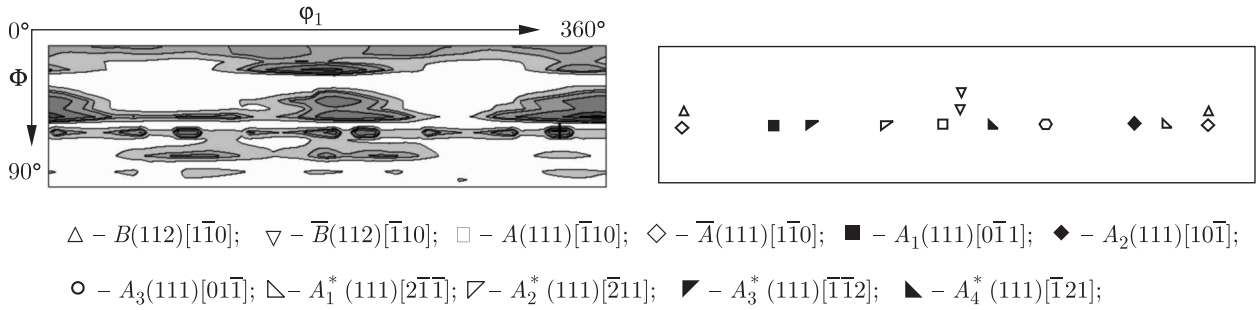

Fig. 4. Experimental ODF (φ_2 = 45° section) for area III of Cu-sample after the 1st HPT rotation (left), and its equivalent with ideal positions of identified orientations (right) given bottom

{hkl}<110>. However, the maxima of the experimental texture are observed to deviate slightly (≈10°) from their corresponding ideal positions. The reason is most probably in the asymmetry flow of material during the HPT. A similar effect was observed earlier in the case of ECAP for Cu [12].

The calculated volume fractions of the texture maxima close to the ideal orientations identified in the examined sample are presented in Tab. 2. The data concern the measurement points (I, II and III) for the sample after the first HPT-rotation, as well as one selected point for samples after 1-, 5- and 10 rotations.

The results presented in Tab. 2 show that in the investigated area (I) the maximal volume fraction is that belonging to the texture components C and A^* after the 1st rotation. These components decreased at higher deformation at points II and III, while the intensity of the A and B components increased. The observed changes of the texture components distant from the centre of the sample (correlated with various ideal orientations of simple shearing) resulted from the various deformation degrees and the different active slip systems. The results correspond to those investigated by means of the SEM EBSD technique [29]. The number of the rotations realized in the HPT in-

creases, while the intensity of dominating texture components decreases. This effect is connected with increasing contribution of grain boundaries at higher deformation degrees [30]. An ultra-fine structure has formed after the 5^{th} rotation of the HPT, when high-angle boundaries are intensively generated in the material [31].

Table 1
The main texture components of simple shearing for metals with cubic lattice symmetry [21]. Indices (hkl) correspond to the lattice planes parallel to shearing planes and [uvw] denote crystallographic axis parallel to shearing direction

Symbol	hkl<uvw>	Symbol	hkl<uvw>
A_1^*	(111)[$2\bar{1}\bar{1}$]	B	(112)[$1\bar{1}0$]
A_2^*	(111)[$\bar{2}11$]	$\overline{B}$	(112)[$\bar{1}10$]
A	(111)[$\bar{1}10$]	C	{001}<110>
$\bar{A}$	(111)[$1\bar{1}0$]		

Table 2
Volume fractions of main texture components of Cu samples subjected to the HPT process. 10°-spreading around its ideal position in Euler orientation space $\{\varphi_1, \Phi, \varphi_1\}$ was assumed

	Ideal orientations	Volume fractions (vol. %)				
		Point I	Point II	Point III		
		1 rotation			5 rotation	10 rotation
B	(112)[$1\bar{1}0$]	1.77	2.72	3.48	2.39	0.79
	(112)[$\bar{1}10$]	1.29	2.00	3.27	1.19	0.99
A	(111)[$\bar{1}10$]	1.94	2.10	2.83	0.58	1.32
	(111)[$1\bar{1}0$]	2.21	2.24	2.56	2.09	1.62
A^*	(111)[2 $\bar{1}\bar{1}$]	1.91	1.92	1.62	1.73	1.47
	(111)[$\bar{2}$ 1 1]	1.75	2.20	1.85	1.20	1.31
C	(100)[$0\bar{1}$ 1]	2.91	2.62	2.15	1.82	1.09

The obtained results point to the fact that the texture maxima correspond to the ideal orientations of simple shear in the centre of the deformed samples as well as along their radii. The analysis of the character of the material flow points to the fact that parts of the material move from the center to the periphery of the sample during the HPT process in the open anvils. At that, the compressive stress (in the centre) or the tensile stresses (in the periphery) apply to simple shear [32]. The movement of the chosen elementary volumes occurs along the spiral trajectory. Apparently, this fact may influence the orientation of the texture maxima in relation to the preferred direction in sample space.

In the considered case of the textures after the 1^{st} rotation, the angle, by which the maxima had to be rotated on the PF till the coincidence with the ideal orientations of simple shear, was 53° for the central sample area and 40°, and 30° for areas II- and III-, respectively. It is known that at the initial stages of rolling strain bands are inclined at an angle α to the rolling plane [12]. With the strain degree rising, the strain bands rotating to the rolling plane. In our case different degrees of the accumulated strain correspond to HPT areas, which are situated at different distances from the rotation axis of the anvils. If simple shear takes place inside the band, then additional rotation of the strain band in relation to the sample axes will be different and decreasing while moving away from the rotation axis, as at the same time the strain degree increases. Such a supposition corresponds to the experimentally observed regularities of texture formation in case of Cu, subjected to HPT.

3.2. Texture evolution in ECA pressing. In Fig. 5 experimental PFs and ODFs are presented, which show the evolution of the crystallographic texture of Cu sample during the 1^{st} ECAP pass.

The manner of arrangement of main texture maxima points to the fact that formation of textures, typical of simple shear, takes place in the area of intersection of the die-set channels (Figs. 1 and 5, area 4) [11]. This is confirmed by the presence of practically all the texture components, which are ideal crystallographic orientations of the simple shear textures (Tab. 1, Fig. 5). The given crystallographic orientations are rotated by 45° counterclockwise [11].

At the same time, the texture components A_θ, $A_{1\theta}^*$ and $A_{2\theta}^*$ have maximal intensity and the rest of the ideal orientations are expressed slightly (Tab. 4). During metal flow in the space of the horizontal channel the crystallographic texture is still changing (Fig. 5, areas 5–7). The results of the calculation of the volume fraction of the ideal orientations show that the intensity of texture maxima A_θ, $A_{1\theta}^*$, $A_{2\theta}^*$, $\bar{A}_\theta$ and B_θ increases, and the intensity of the texture maxima $\bar{B}_\theta$ and C_θ decreases. The changes of the crystallographic texture in the horizontal channel confirm the evaluation of the texture index (Tab. 5). The calculation results show that after passing through the plane of the channels' intersection the texture intensifies. This may be connected with the fact that there was no backpressure in the experiment. The material layers, which are located in a distance of the billet tail, push the layers, which have already passed, when moving through the plane of the channels' intersection. This leads to additional straining and intensifies the crystallographic texture. The predominance of the orientations A_θ, $A_{1\theta}^*$, $A_{2\theta}^*$, $\bar{A}_\theta$ after the 1^{st} ECAP pass corresponds to the results of experiments presented in [33].

The rotation of main texture maxima about the axis z by 10° counterclockwise takes place, and the shift of the maxima are observed on the ODF (Fig. 5g). The most probable cause of the change of the texture of the material, that passed the zone of the channels' intersection, where simple shear takes place, is activization of non-shear deformation modes. That may be conditioned by the friction effect between a billet and the walls of the horizontal channel.

Table 3
Main ideal crystallographic orientations of the simple shear textures in case of *fcc*-metals [11]. The index (hkl) is used to designate the planes, parallel to the shear plane, and the index [uvw] is used for the crystallographic directions, oriented along shear direction

Symbol	hkl<uvw>	Symbol	hkl<uvw>
$A_{1\theta}^*$	(81$\bar{1}$)[1$\bar{4}\bar{4}$]	B_θ	(312)[15$\bar{4}$]
$A_{2\theta}^*$	(353)[55$\bar{6}$]	$\bar{B}_\theta$	($\bar{1}\bar{5}$4)[3$\bar{1}\bar{2}$]
A_θ	(914)[$\bar{1}$11$\bar{5}$]	C_θ	{334}<22$\bar{3}$>
$\bar{A}_\theta$	(11$\bar{1}$5)[$\bar{9}\bar{1}$4]		

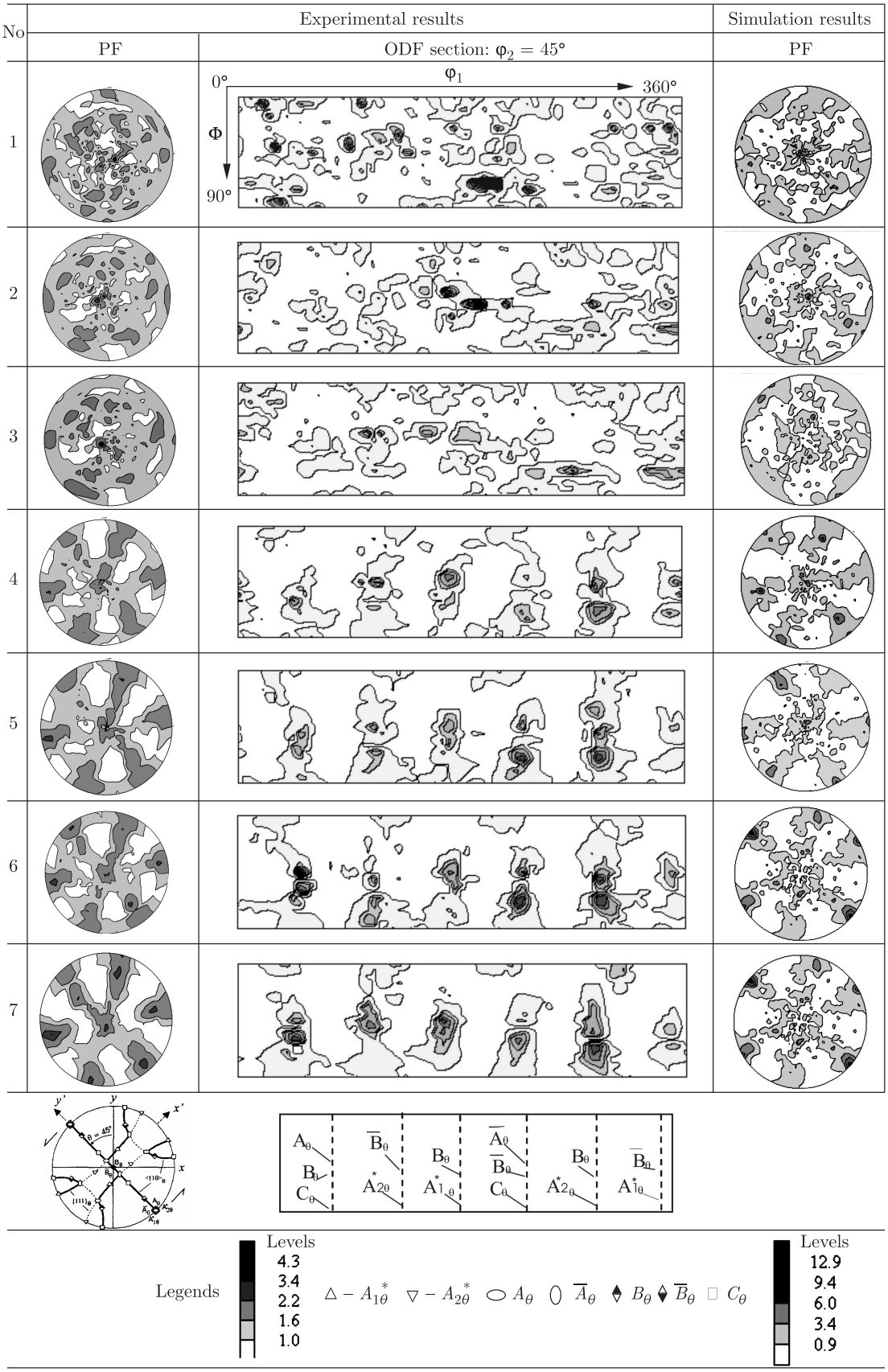

Fig. 5. The rows present experimental and simulated results; PFs (111) and ODFs ($\phi_2 = 45°$) received for the investigated areas 1–7 (marked in Fig. 1) for the 1st ECAP pass and the arrangement of the ideal orientations of the simple shear textures after rotating by the angle 45° counterclockwise [11]. The axis x' belongs to the shear plane (the plane of channels' intersection)

Table 4
The experimental and model values of the volume fraction of main texture components for fcc metals during the 1st ECAP pass. The assumed spreading around of Euler angles was 10°

Investigated sample area	Volume fractions (vol. %)													
	A_θ		$A^*_{1\theta}$		$A^*_{2\theta}$		$\bar{A}_\theta$		B_θ		$\bar{B}_\theta$		C_θ	
	Exp.	Mod.	Exp.	Mod.	Exp.	Mod.	Exp.	Mod.	Exp.	Mod.	Exp.	Mod.	Exp.	Mod.
1	1.57	2.29	2.23	0.80	0.79	2.59	2.23	0.80	0.78	1.75	1.09	0.10	1.64	0.92
2	2.22	0.19	2.09	0.39	1.61	1.22	1.95	1.33	2.71	0.46	2.05	0.85	1.10	0.48
3	1.67	1.61	1.58	1.30	1.67	1.61	1.58	1.30	1.86	1.34	2.15	1.53	0.97	0.75
4	3.42	4.08	3.53	4.41	3.53	4.44	2.11	1.89	2.93	1.56	2.20	1.94	0.79	0.85
5	4.03	3.90	4.05	3.96	4.05	3.96	2.33	2.84	2.46	1.47	2.79	1.96	1.07	1.24
6	4.67	3.44	4.83	3.88	4.72	3.44	2.66	2.67	2.66	1.61	2.78	1.90	1.17	1.25
7	5.21	2.55	5.01	2.55	5.73	3.29	3.72	2.67	3.02	1.01	2.28	1.92	0.75	1.02

Table 5
The value of the texture index for experimental textures during the 1st ECAP pass

Investigated sample area	1	2	3	4	5	6	7
Texture index	2.7	2.5	2.5	2.5	2.8	3.2	3.5

In order to prove this assumption computer simulation of the crystallographic textures has been carried out with the change of the stress-strain state of the material taken into account in the process of ECAP [23]. The simulation results are presented in Fig. 5.

The comparison with the experimental PFs has shown that the simulated results reflect the real processes of texture formation, which take place in material (Fig. 5). In particular, the PF, corresponding to the plane of the channels' intersection, in which simple shear takes place, are completely identical (Fig. 5, area 4). The results of the calculation of the volume fraction of the ideal orientations show that the orientations A_θ, $A^*_{1\theta}$, $A^*_{2\theta}$ have maximal intensity (see Tab. 4). When moving along the horizontal channel, the weakening of the intensity of the most texture maxima occurs. At that, experimentally observed rotation of the texture maxima is clearly noticeable on the model PFs for the investigated areas 5–7 (Fig. 5).

By the model the changes of the strain rate gradient components while passing through the control area in a billet is presented in Figs. 6 and 7. The presented graphs show that formation of these components takes place in the area adjacent to the plane of channels' intersection. The activity of the shear components of the strain rate gradient starts earlier than that of the compression and tensile components (Figs. 6 and 7). The formation of the crystallographic texture in the plane of intersection of the die-set channels (Fig. 5) is accompanied by the activity of the shear components, which act along the plane of the channels' intersection. The compression component acts along the vertical channel and the tensile component acts along the horizontal channel (Figs. 6 and 7). When moving through the horizontal channel, insignificant change of the shear components, the strain rate gradient, the compression and tensile components take place. In their turn they may result in the change of the volume fraction of the ideal orientations and in the rotation of the maxima on the PFs.

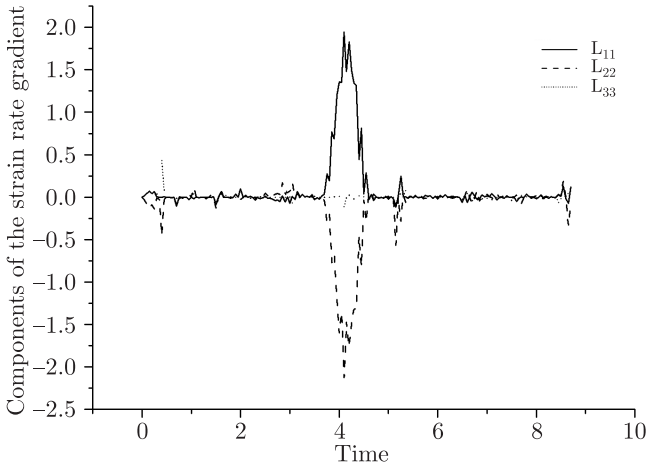

Fig. 6. The dependence of the strain rate gradient components on time during the 1st ECAP pass ($i = j$)

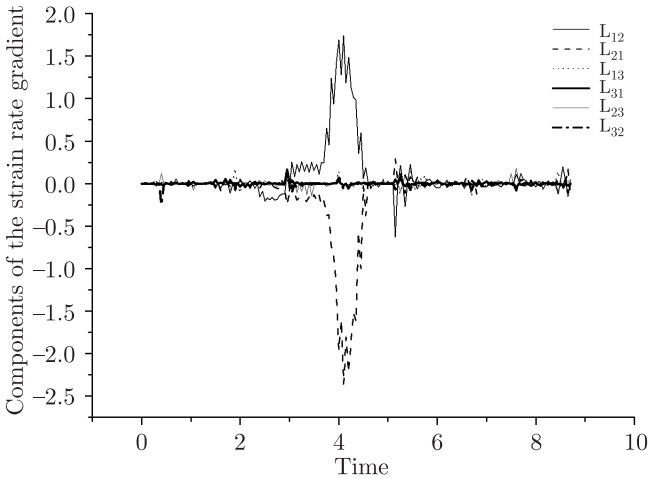

Fig. 7. The dependence of the strain rate gradient components on time during the 1st ECAP pass ($i \neq j$)

Besides the mentioned similarities the crystallographic textures, obtained by experiment and simulation, have also a number of important differences. First, the intensity of texture maxima in the model PF is much higher than the intensity of the experimentally determined maxima. Second, during the metal

flow in the horizontal channel, the calculation results of the volume fraction show, that in the experiment the increase of the volume fraction of the main texture maxima takes place it decrease in the simulation. One of the possible reasons is the influence of friction on the character of the crystallographic texture. During the experiments, when the billet passes through the die, the character of the friction coefficient may change, as the material squeezes the lubricant. During simulation the value of the friction coefficient is constant. This fact can influence the character of the simulated textures. Besides, when modelling the formation of deformation bands, their rotation are not taken into account. Only dislocation slip in the grain body is considered. The attempts to solve the problem have been made in [34].

3.3. Experimental studies of texture heterogeneity during increase of the number of passes. The experimental studies of heterogeneity of the crystallographic texture at more than one pass were carried out for the route $\mathrm{B_C}$. The choice of this ECAP route was conditioned by the fact that it results in the maximal structure refinement [35].

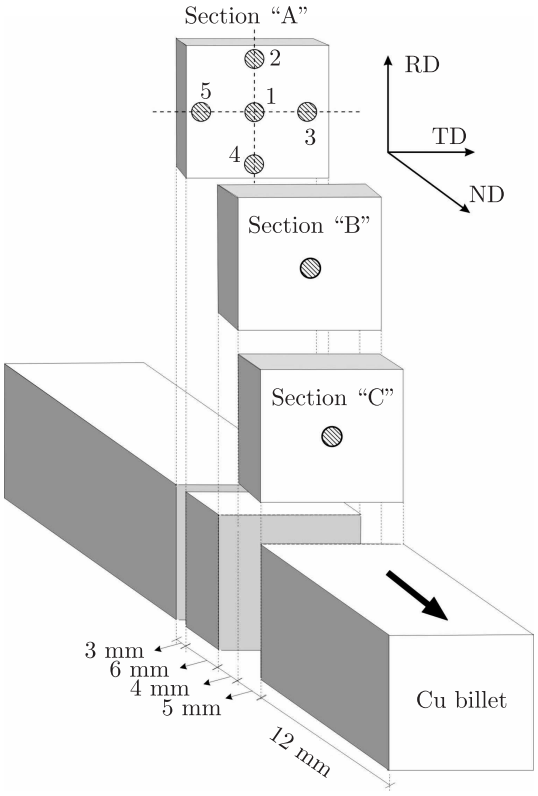

Fig. 8. The scheme of cutting out a billet for investigation of its texture heterogeneity

The scheme of cutting out a billet for the investigation of the heterogeneity of the crystallographic texture is presented in Fig. 8. Only the cross section A was studied in the given paper. When investigating the heterogeneity of the crystallographic texture in the examined section, 5 selected points have been studied. The choice of the points for investigation was conditioned by 2 factors: (i) by the necessity to describing the heterogeneity of the texture completely, (ii) by the results of modelling the material flow, which point at the heterogeneous character of strain distribution over the cross section of a billet during ECAP.

The results of the investigation are presented as complete PFs in Fig. 9. The volume fraction of the main texture maxima (Tab. 6), the values of the texture index, an average value of the texture index $< T >$ and the mean-square deviation of the texture index (ΔT^2) (Tab. 7) were calculated for quantitative analysis. As it is seen from Fig. 10, some definite heterogeneity of texture along the cross section of a billet takes place in the initial state. The PFs, however, are characterized by rather randomly arranged maxima.

After the 1$^{\mathrm{st}}$ pass rather one-type textures form in the investigated areas No 1, 2, 3 and 5 (Tab. 7). The results of the calculation of the texture index show that the most blurred texture forms in area No 4 (Tab. 7). Results of the material flow modelling show an undeformed zone of the material. It is observed in the lower part of a billet, which is possibly the cause of such distribution of the texture maxima [22]. After the 1$^{\mathrm{st}}$ pass the formed texture may be described with the help of ideal orientations, presented in Fig. 10. The mentioned ideal orientations were obtained by rotating the ideal orientations of simple shear by 45° counterclockwise around the TD axe in Fig. 8. At that, the orientations A_θ, $A^*_{1\theta}$ and $A^*_{2\theta}$ have maximal intensity.

Table 6
The experimental data of the volume fraction of main texture components during the 1$^{\mathrm{st}}$ ECAP pass. The spreading along Euler's angles was 10°

Investigated sample area		Volume fraction of the orientations						
		A_θ	$A^*_{1\theta}$	$A^*_{2\theta}$	$\bar{A}_\theta$	B_θ	$\bar{B}_\theta$	C_θ
As-recived	No 1	0.38	0.35	0.36	1.24	0.74	1.58	0.34
	No 2	1.19	0.34	0.36	2.75	2.61	0.74	0.53
	No 3	0.4	0.57	0.98	0.53	0.97	1.39	0.95
	No 4	0.34	0.29	0.47	0.23	1.04	1.19	0.53
	No 5	0.97	0.37	0.45	0.84	1.44	1.22	0.65
1 pass	No 1	0.63	1.27	2.68	0.3	1.77	3.1	2.58
	No 2	1.62	0.92	2.23	0.67	3.16	3.41	2.23
	No 3	0.9	0.86	1.9	0.19	1.92	3.26	2.59
	No 4	0.39	0.22	0.75	0.58	1.14	3.11	0.6
	No 5	1.01	1.68	1.7	0.11	3.48	3.39	1.6
2 pass	No 1	0.25	0.56	0.79	0.77	0.51	2.14	0.53
	No 2	1.02	0.78	0.42	1.07	1.00	1.58	0.36
	No 3	0.35	0.5	1.15	0.5	0.56	1.55	0.7
	No 4	0.36	0.28	0.42	0.77	0.88	2.68	0.32
	No 5	1.01	0.13	0.35	0.59	0.66	2.61	0.27
4 pass	No 1	0.32	0.57	0.76	0.57	1.12	4.73	0.58
	No 2	0.34	0.78	1.81	0.78	1.52	4.64	1.42
	No 3	0.49	0.06	1.41	1.15	1.22	1.39	0.67
	No 4	0.62	0.06	0.84	0.73	0.45	2.61	0.4
	No 5	0.7	0.35	0.44	0.26	1.79	2.98	0.22
12 pass	No 1	0.42	0.32	0.22	1.56	0.36	1.98	0.18
	No 2	0.71	0.32	0.37	1.67	0.55	1.74	0.34
	No 3	0.33	0.08	0.34	2.42	0.63	1.38	0.22
	No 4	0.73	0.18	0.37	0.79	1.04	3.49	0.31
	No 5	0.37	0.25	0.74	0.85	0.85	3.43	0.36

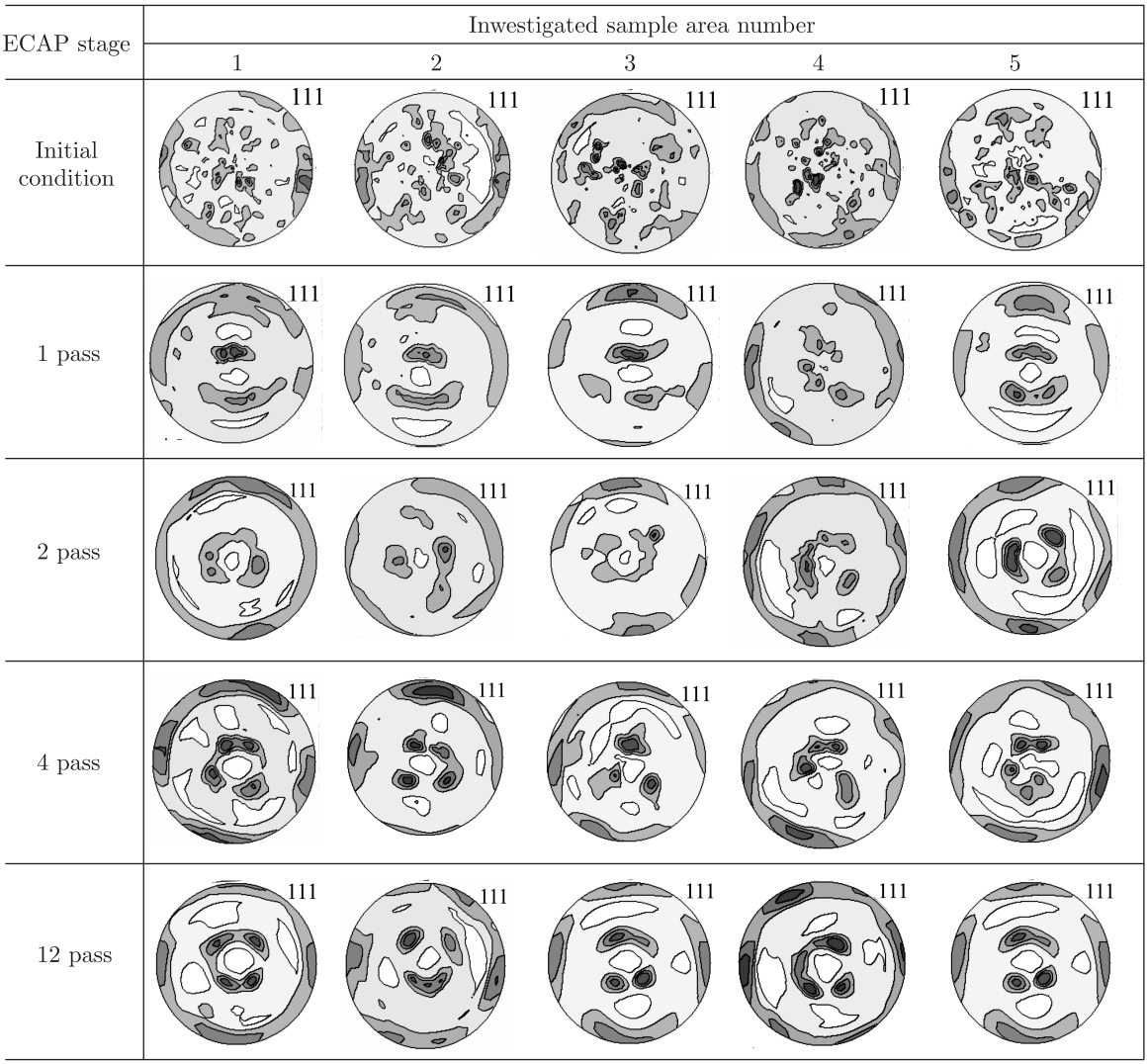

Fig. 9. Heterogeneity of the crystallographic texture at different stages of ECAP. Areas 1–5 correspond to Fig. 8. Pole figure levels: 0.4, 1.2, 1.9, 2.7, 5.3, 6.2

Table 7
The value of the texture index, average value of the texture index <T> and mean-square deviation of the texture index (ΔT^2) for experimental textures during the 1, 2, 4 and 12 ECAP passes (route Bc). Areas No 1–5

ECAP stage	Value of the texture index (T)					$< T >$	(ΔT^2)
	No 1	No 2	No 3	No 4	No 5		
As-received	3.1	4.1	2.4	2.5	3.3	3.08	0.68
1 pass	2	2.8	2	1.7	1.9	2.08	0.42
2 pass	2.5	1.6	1.6	3.1	3.5	2.46	0.86
4 pass	4.9	2.5	2.6	2.5	2.7	3.04	1.04
12 pass	3.2	3.7	2.9	4.5	3.8	3.62	0.61

The widest scattering in the values of the texture index is observed in the 2$^{\rm nd}$ and 4$^{\rm th}$ ECAP passes. At that, in the 2$^{\rm nd}$ ECAP pass the least expressed texture is observed in points 2 and 3. After the 4$^{\rm th}$ and 12$^{\rm th}$ passes the textures in the cross-section are very similar. Possibly it is connected with the 4-pass cycling (4×90° = 360°) in the cases. After the 4$^{\rm th}$ and 12$^{\rm th}$ passes the formed crystallographic texture is characterized by the predominance of the orientations B_θ and $\bar{B}_\theta$.

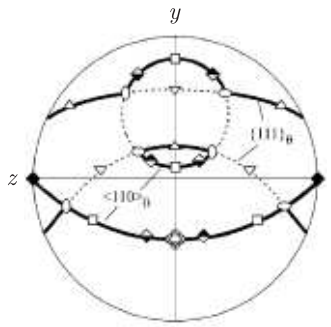

$\triangle - A_{1\theta}^{*}$ $\triangledown - A_{2\theta}^{*}$ $\bigcirc A_\theta$ $\bigcirc\!\!\!\!-\ \overline{A}_\theta$ $\blacklozenge B_\theta$ $\blacklozenge\!\!\!\!-\ \overline{B}_\theta$ $\square\ C_\theta$

Fig. 10. Arrangement of the ideal orientations of ECA pressing from the cross section of the billet

The analysis shows, that the average value of the texture index in the cross section of the initial state is rather high with rather wide scatter. During the 1^{th} pass it decreases and the texture becomes more homogeneous. The increase of the number of passes from 1 to 12 is characterized by the growth of the texture index, the heterogeneity of the texture grows from 1 to 4 pass. The comparison of the results of the 4 and 12 passes points to the increase of the texture heterogeneity.

4. Conclusions

As a result of the conducted investigations, it was shown that during HPT and ECAP crystallographic textures form, which may be described with the help of the ideal orientations of the simple shear. At the initial stages of HPT the texture sharpness increases as far as the points under consideration are distancing from the rotational axis. Blurring of the texture maxima are observed with further increase in the number of rotations. The rotation of the texture maxima with respect to the positions of the ideal orientations can be explained by the formation of deformation bands, oriented to the billet's axes differently at different strain degrees.

The main texture formation processes during the 1^{th} ECAP pass take place in the zone, adjacent to the plane of the die-set channels' intersection. However, even in the horizontal outlet channel some texture enforcement is observed. The analysis of the experimental results with the help of computer simulations points to the activization of definite slip systems, which provides simple shear and the effect of compressive and tensile deformation modes as well. In case of ECAP the increase of the number of passes results in tendency to increase of the texture sharpness. The homogeneity of the texture increases up to the 4^{th} pass, then it begins to decrease.

Acknowledgements. This study was conducted within the framework of CRDF project 10505 "Model-driven manufacturing of nanocrystalline structure" (the project coordinator – Dr. I.J. Beyerlein). The work was also supported by:

– RFBR project 05-08-49967a "Development of scientific technology basis for producing of bulk nanomaterials during equal-channel angular pressing",
– "MMC", OJSC, ETC "Ausferr" and "Intels" Foundation of Science and Education (grant No. 19-04-02), Russia,
– Ministry of Scientific Research and Information Technology ("Topography of crystollographic texture with the use of Roentgen's diffraction technique", grant No. 3 T08C 064 26), Poland.

REFERENCES

[1] R.Z. Valiev, R.K. Islamgaliev, and I.V. Alexandrov, "Bulk nanostructured materials from severe plastic deformation", *Prog. Mat. Sci.* 45, 103 (2000).

[2] O.V. Mishin, V.Y. Gertsman, R.Z. Valiev, and G. Gottstein, "Grain boundary distribution and texture in ultrafine grained copper produced by severe plastic deformation", *Scripta Mater.* 35, 873 (1996).

[3] I.V. Alexandrov, A.A. Dubravina, A.R. Kilmametov, V.U. Kazyhanov, and R.Z. Valiev, "Textures in nanostructured metals processed by severe plastic deformation", *Metals and Materials Int.* 9, 151 (2003).

[4] V.M. Segal, "Equal channel angular extrusion: from macromechanics to structure formation", *Mater. Sci. Eng.* A 271, 322 (1999).

[5] Y. Iwahashi, J. Wang, Z. Horita, M. Nemoto, and T.G. Langdon, "Principle of equal channel angular pressing for the processing of ultra-fine grained materials", *Scripta Mater.* 35, 143 (1996).

[6] P.W. Bridgman, *Studies in Large Plastic Flow and Fracture*, McGraw-Hill, New-York, 1952.

[7] A.V. Korznikov, Y.V. Ivanisenko, D.V. Laptionok, I.M. Safarov, V.P. Pilyugin, and R.Z. Valiev, "Influence of severe plastic deformation on structure and phase composition of carbon steel", *NanoStructured Materials* 4, 159 (1994).

[8] I.V. Alexandrov, A.A. Dubravina, and H.S. Kim, "Nanostructure formation in copper subjected to high-pressure torsion", *Defect and Diffusion Forum* 208–209, 229 (2002).

[9] A. Vorhauer and R. Pippan, "On the homogeneity of deformation by high pressure torsion", *Scripta Mater.* 51, 921 (2004).

[10] M.J. Zehetbauer, H.P. Stuwe, A. Vorhauer, E. Schafler, and J. Kohout, "The role of hydrostatic pressure in Severe plastic deformation", *Advan. Engin. Mater.* 5, 330 (2003).

[11] S. Li, I.J. Beyerlein, and M.M. Bourke, "Texture formation during ECAE of fcc and bcc materials: comparison with simple shear", *Mater. Sci. Eng.* A 394, 66 (2005).

[12] L.S. Tóth, R.A. Massion, L. Germain, S.C. Baik, and S. Suwas, "Analysis of texture evolution in equal channel angular extrusion of copper using a new flow field", *Acta Mater.* 52, 1885 (2004).

[13] L.S. Toth, "Texture evolution in severe plastic deformation by equal channel angular extrusion", *Proc. of the 2^{nd} Inter. Conf. on Nanomaterials by Severe Plastic Deformation: Fundamentals – Processing – Applications – NanoSPD2*, Wien, 281 (2002).

[14] E.F. Rauch and L. Dupuy, "Textural evolution during equal channel angular extrusion versus planar simple shear", *Proc. of the 2^{nd} Inter. Conf. on "Nanomaterials by Severe Plastic Deformation: Fundamentals – Processing – Applications – NanoSPD2*, Wien, Austria, 297 (2002).

[15] J.T. Bonarski, I.V. Alexandrov, and L. Tarkowski, "Development of crystallographic texture and microstructure in Cu and Ti, subjected to equal-channel angular pressing", *Proc. of the 2^{nd} Inter. Conf. on Nanomaterials by Severe Plastic Deformation: Fundamentals – Processing – Applications – NanoSPD2*, Wien, 315 (2002).

[16] A. Gholinia, P.Bate, and P.B. Prangnell, "Modelling texture development during ECAE of Aluminium", *Acta Mater.* 50, 2121 (2002).

[17] J. Qin, H. Jun-Hyun, Z. Guoding, and Jae-Chul Lee, "Characteristic of texture evolution induced by equal channel angular pressing in 6061 aluminum sheets", *Scripta Mater.* 51, 185 (2004).

[18] W.Q. Cao, A. Godfrey, and Q. Liu, "EBSP investigation of microstructure and texture evolution during equal channel angular pressing of aluminium", *Mater. Sci. Eng.* A 361, 9 (2003).

[19] I.J. Beyerlein, R.A. Lebensohn, and C.N. Tóme, "Modelling texture and microstructural evolution in the equal channel angular extrusion process", *Mater. Sci. Eng.* A 345, 122 (2003).

[20] T.R. McNelley, D.L. Swisher, Z. Horita, and T.G. Langdon, "Influence of processing route on microstructure and grain bound-

ary development during equal-channel angular pressing of pure aluminum", *Proc. of Ultra fine grained materials II*, ed. Y.T. Zhu, T.G. Langdon, R.S. Mishra, S.L. Semiatin, M.J. Saran and T.C. Lowe in: *The Minerals, Metals and Materials Society*, 505 (2002).

[21] U.F. Kocks, C.N. Tome, and H.R. Wenk, *Texture and Anisotropy: Preferred Orientations in Polycrystals and their Effect*, 676 Cambridge University Press, Cambridge, (1998).

[22] I.V. Alexandrov, I.N. Budilov, G. Krallics, H.S. Kim, S.C. Joon, A.A. Smolyakov, A.I. Korshunov, and V.P. Solovyev, "Simulation of equal channel angular extrusion", *Proc. of the* 3^{rd} *International Conference on Nanomaterials by Severe Plastic Deformation*, Fukuoka, Japan, 201 (2005).

[23] I.V. Alexandrov, M.V. Zhilina, A.V. Scherbakov, A.I. Korshunov, P.N. Nizovtsev, A.A. Smolykov, V.P. Solovyev, I.J. Beyerlein, and R.Z. Valiev, "Formation of crystallographic texture during severe plastic deformation", *Archives of Metallurgy and Materials* 50 (2), 281 (2005).

[24] L.S. Tóth, "Modelling of strain hardening and microstructural evolution in ECAP", *Computational Mater. Science* 32, 568 (2005).

[25] S. Li, I.J. Beyerlein, D.J. Alexander, and S.C. Vogel, "Texture evolution during multi-pass equal channel angular extrusion of copper: Neutron diffraction characterization and polycrystal modelling", *Acta Mater.* 53, 2111 (2005).

[26] C.N. Tome, G.R. Canova, U.F. Kock, N. Christodoulou, and J.J. Jonas, "The relation between macroscopic and microscopic strain hardening in F.C.C. polycrystals", *Acta Metal.* 32 (10), 1637 (1984).

[27] A.I. Abakumov, A.V. Pevnitsky, V.P. Solovyev, and I.V. Zbababakhin, "DRAKON code for 2D and 3D simulations of elastic-plastic flows under shock-wave load", in: *Scientific Readings. Proceedings of the Intern. Conf.*, Snezhinsk, Russia, 227 (1995).

[28] K. Pawlik and P. Ozga, *LaboTex*: *The Texture Analysis Software*, "Göttinger Arbeiten zur Geologie und Paläontologie", SB4 (1999).

[29] M.J. Zehetbauer, J. Kohout, E. Schafler, F. Sachslehner, and A.A. Dubravina, "Plastic deformation of nickel under high hydrostatic pressure", *J. Alloys and Compounds* 378, 329 (2004).

[30] E.V. Kozlov, A.N. Zhdanov, L.N. Ignatenco, N.A. Popova, Yu.F. Ivanov, and N.A. Koneva, "Structural evolution of ultrafine-grained copper and copper-based alloy during plastic deformation", *Proceedings of 2002 TMS Annual Meeting in Seattle*, Washington, 419 (2002).

[31] A.N. Tyumentsev, Yu.P. Pinzhin, M.V. Tretyak, A.D. Korotaev, I.A. Ditenberg, R.Z. Valiev, R.K. Islamgaliev, and A.V. Korznikov, "Evolution of defect substructure of metal alloys at microscopic and mesoscopic level under torsion", *Theoret. Appl. Fracture Mechanics* 35, 155 (2001).

[32] H.S. Kim, S.I. Hong, Y.S. Lee, A.A. Dubravina, and I.V. Alexandov, "Deformation behaviour of copper during a high pressure torsion process", *J. Materials Processing Technology* 142, 334 (2003).

[33] A.A. Gazder, F.D. Torre, C.F. Gu, C.H.J. Davies, and E.V. Pereloma, "Microstructure and texture evolution of bcc and fcc metals subjected to equal channel angular extrusion", *Mater. Sci. Eng.* A 415, 126-139 (2006).

[34] M. Seefeldt and P.V. Houtte, "Grain subdivision and local texture evolution studied by means of a coupled substructure-texture evolution model", *Materials Science Forum* 408–412, 433 (2002).

[35] M. Furukawa, Y. Iwahashi, Z. Horita, M. Nemoto, and T.G. Langdon, "The shearing characteristics associated with equal-channel angular pressing", *Mater. Sci. Eng.* A 257, 328 (1998).